Developmental Biology 374 (2013) 71–84

Contents lists available at SciVerse ScienceDirect

Developmental Biology

journal homepage: www.elsevier.com/locate/developmentalbiology

Multi-modal effects of BMP signaling on *Nodal* expression in the lateral plate mesoderm during left–right axis formation in the chick embryo

Kenjiro Katsu [a], Norifumi Tatsumi [b], Daisuke Niki [c], Ken-ichi Yamamura [c], Yuji Yokouchi [c,*]

[a] Division of Pattern Formation, Department of Organogenesis, Institute of Molecular Embryology and Genetics, 2-2-1 Honjo, Chuo-ku, Kumamoto 860-0811, Japan
[b] Department of Anatomy, The Jikei University School of Medicine, 3-25-8 Nishishinbashi, Minato-ku, Tokyo 105-8461, Japan
[c] Division of Developmental Genetics, Institute of Resource Development and Analysis, Kumamoto University, 2-2-1 Honjo, Chuo-ku, Kumamoto 860-0811, Japan

ARTICLE INFO

Article history:
Received 12 January 2012
Received in revised form
26 November 2012
Accepted 26 November 2012
Available online 1 December 2012

Keywords:
Nodal
BMP
Noggin
Left–right asymmetry
Chick

ABSTRACT

During development of left–right asymmetry in the vertebrate embryo, *Nodal* plays a central role for determination of left-handedness. Bone morphogenetic protein (BMP) signaling has an important role for regulation of *Nodal* expression, although there is controversy over whether BMP signaling has a positive or negative effect on *Nodal* expression in the chick embryo. As BMP is a morphogen, we speculated that different concentrations might induce different responses in the cells of the lateral plate mesoderm (LPM). To test this hypothesis, we analyzed the effects of various concentrations of BMP4 and NOGGIN on *Nodal* expression in the LPM. We found that the effect on *Nodal* expression varied in a complex fashion with the concentration of BMP. In agreement with previous reports, we found that a high level of BMP signaling induced *Nodal* expression in the LPM, whereas a low level inhibited expression. However, a high intermediate level of BMP signaling was found to suppress *Nodal* expression in the left LPM, whereas a low intermediate level induced *Nodal* expression in the right LPM. Thus, the high and the low intermediate levels of BMP signaling up-regulated *Nodal* expression, but the high intermediate and low levels of BMP signaling down-regulated *Nodal* expression. Next, we sought to identify the mechanisms of this complex regulation of *Nodal* expression by BMP signaling. At the low intermediate level of BMP signaling, regulation depended on a NODAL positive-feedback loop suggesting the possibility of crosstalk between BMP and NODAL signaling. Overexpression of a constitutively active BMP receptor, a constitutively active ACTIVIN/NODAL receptor and SMAD4 indicated that SMAD1 and SMAD2 competed for binding to SMAD4 in the cells of the LPM. *Nodal* regulation by the high and low levels of BMP signaling was dependent on *Cfc* up-regulation or down-regulation, respectively. We propose a model for the variable effects of BMP signaling on *Nodal* expression in which different levels of BMP signaling regulate *Nodal* expression by a balance between BMP-pSMAD1/4 signaling and NODAL-pSMAD2/4 signaling.

Introduction

Nodal plays important roles in patterning of the primary body axis of the vertebrate embryo (Hamada et al., 2002; Shen, 2007; Tabin, 2006). NODAL binds to type I and type II receptors, which signal to the nucleus through SMAD2/SMAD3 and SMAD4 complexes. NODAL can regulate downstream genes only in the presence of co-receptors of the *Cfc* family.

In the vertebrate embryo, *Nodal* plays a central role as a left determinant for patterning the left–right (L–R) axis. In mice, *Nodal* is expressed in perinodal crown cells and is then transferred to the left lateral plate mesoderm (LPM), resulting in asymmetric, left-handed expression of *Nodal* (Hamada et al., 2002; Shiratori and Hamada, 2006). Perinodal expression of *Nodal* is responsible for *Nodal* expression in the left LPM. In the LPM, NODAL activates its own transcription by a positive feedback mechanism in a *Cfc* and *FoxH1* dependent manner. NODAL induces *Lefty-1* and *-2*, which act as negative regulators of NODAL and restrict NODAL activity to the left side of the body. NODAL also induces a left-specific transcription factor *Pitx2* that is implicated in the control of internal organ morphology.

There is increasing evidence that bone morphogenetic proteins (BMPs) also have a role in the regulation of L–R axis formation, although the conclusions of the various reports are not completely consistent. Some studies have reported that BMP signaling has a negative effect on *Nodal* expression (Chang et al., 2000; Kishigami et al., 2004; Rodriguez Esteban et al., 1999; Yokouchi et al., 1999), other studies suggest that it has a positive effect (Fujiwara et al., 2002; Piedra and Ros, 2002; Schlange et al., 2002; Yu et al., 2008). Recently, supportive evidence for a negative role

* Corresponding author. Fax: +81 96 373 6625.
E-mail address: yokouchi@kumamoto-u.ac.jp (Y. Yokouchi).

0012-1606/$ - see front matter © 2012 Elsevier Inc. All rights reserved.
http://dx.doi.org/10.1016/j.ydbio.2012.11.027

for BMP signaling was obtained in the mouse. Phosphorylated SMAD1/5/8 is less abundant in the left LPM and this asymmetric distribution is attributed to BMP inhibition by NOGGIN and Chordin whose expression is enriched in the left LPM (Mine et al., 2008). The conditional deletion of *Smad1* in the LPM confirmed a repressive role for BMP signaling (Furtado et al., 2008). In contrast to the mouse embryo, the role of BMP signaling in the regulation of *Nodal* expression during chick L–R axis formation is still unclear. In chick embryos, BMP signaling has been reported to have a negative influence on *Nodal* expression on the basis that the *Cerberus*/*DAN* family member *Cerberus*/*Caronte* is expressed in the left LPM and induces *Nodal* expression by inhibition of BMP signaling (Rodriguez Esteban et al., 1999; Yokouchi et al., 1999; Zhu et al., 1999). By contrast, a positive role for BMP signaling has been suggested from the observation that application of BMP to the LPM up-regulates *Nodal* expression whereas NOGGIN down-regulates expression (Piedra and Ros, 2002; Schlange et al., 2002). This apparent inconsistency currently precludes a definitive understanding of the role of BMP signaling during L–R axis formation in the chick embryo.

In an attempt to reconcile the contradictory conclusions described above on the role of BMP signaling in the chick embryo, we hypothesized that different concentrations of BMP might have different effects in the regulation of *Nodal* expression. Some morphogens are known to have a dose-dependent effect on the level of gene expression in particular developmental pathways (Affolter and Basler, 2007; Mizutani et al., 2006). BMP is also a morphogen and, therefore, different concentrations might induce different responses in the LPM. In the present study, we examined the responses induced by four levels of BMP signaling on *Nodal* expression in the LPM of chick embryos. We found that BMP signaling modulated *Nodal* expression in a concentration-dependent manner during L–R patterning. Our results suggest that competition between BMP signaling and NODAL signaling regulates *Nodal* expression at intermediate levels of BMP signaling. We propose a model for the variable effects of BMP signaling on *Nodal* expression that accounts for the different effects of different levels of BMP signaling in L–R axis formation in the chick embryo.

Materials and methods

Embryos and experimental manipulations

Embryos were staged using the criteria established by Hamburger and Hamilton (1992) and were cultured using New's method (New, 1955). For bead implantation, Affigel-Blue beads (Bio-Rad) of about 200 μm in diameter were soaked in 1 ng/ml to 10 μg/ml solutions of mouse BMP4 protein (R&D Systems), 25 ng/ml to 10 μg/ml mouse NOGGIN (R&D Systems), or 0.1% BSA/PBS. AG1-X2 beads (Bio-Rad) were soaked in 10 mM SB431542 (Sigma) in DMSO. The beads were implanted as described by Katsu et al. (2012).

Electroporation

The coding sequence of chicken *Cfc* was amplified by reverse transcriptase PCR (RT-PCR) using the primers 5′–GCCATGGTCTGGCGAAAACATGTTAG–3′ and 5′–CGGATCCTCACAACTGCCAGCAGCAAAG–3′; the amplified sequence was cloned into the NcoI-BamHI site of a pSlax21 vector, and then subcloned into the ClaI site of a modified pCAGGS expression vector. The coding sequence of mouse *Smad4* was amplified by RT-PCR using the primers 5′–CCATGGACAATATGTCTATAAC–3′ and 5′–TCAGTCTAAAGGCTGTGGGT–3′; the amplified sequence was cloned into the NcoI-NotI site of a pSlax21 vector, and then subcloned into the ClaI site of a modified pCAGGS expression vector. pCAGGS and pCAGGS-*GFP* were provided by Dr. Takahashi (Nara Institute of Science and Technology). Expression vectors carrying a constitutively active form of the Bmp receptor (pc3-Alk6 (QD)-HA: pc3-*caAlk6*) and the constitutively active form of the Activin/Nodal receptor (pc3-Alk4 (TD)-HA: pc3-*caAlk4*) were provided by Drs. Imamura (Ehime University) and Miyazono (University of Tokyo) (Nakao et al., 1997).

Electroporation was performed as previously described (Granata and Quaderi, 2003). DNA solutions (3–5 mg/ml of pCAGGS for control, 3 mg/ml of pc3-*caAlk4*, 3 mg/ml of pc3-*caAlk6*, 3 mg/ml of pCAGGS-*Cfc*, or 5 mg/ml of pCAGGS-*Smad4*) containing 1 mg/ml pCAGGS-*GFP* vector and 0.1% Fast Green in PBS were placed onto explanted HH4 embryos with a glass capillary. An electric pulse of 5 V, 25 ms was applied three times using a CUY21 electroporator (Tokiwa Science). The positions for gene transfer were selected according to the fate map described by Psychoyos and Stern (1996).

Morpholino oligonucleotides

Morpholino oligonucleotides (MOs) were designed to block translation of Smad1 and Smad2; fluorescein-labeled MOs were obtained from Gene Tools (Philomath, USA). The targeted sequences were as follows: Smad1 MO, 5′–AAACTTGTCACGTTCATGGTGATCC–3′; Smad2 MO, 5′–TGGCAGAATGGATGACATGACTCC–3′. The fluorescein-labeled control morpholino (Gene Tools, Philomath, USA) was used for control experiments. MO solutions (1 mM MO) containing 2 mg/ml pCAGGS vector, 1 mg/ml pCAGGS-*GFP* vector and 0.1% Fast Green in PBS were placed onto explanted HH4 embryos with a glass capillary and electroporated as described above. To assess the efficiency of the Smad1 and Smad2 MOs, embryos were electroporated with MOs and tissue samples of an area approximately $600 \times 600\ \mu m^2$ were excised at HH8 from fluorescein/GFP-positive regions. The explants were homogenized in SDS sample buffer, and subjected to SDS-PAGE and immunoblotting (see below).

Whole-mount in situ hybridization, immunostaining, and TUNEL-labeling

RNA probes for *Shh* and *Nodal* were prepared as described by Levin et al. (1995). A 504 bp fragment of chicken *Cfc* was obtained by RT-PCR using the primers 5′–TCCGTGCCTGTCTTGGTACTGT–3′ and 5′–AGTCGCCATGGATGATGCTG–3′. Whole-mount in situ hybridization was carried out as described by Katsu et al. (2012) using digoxigenin-labeled RNA probes.

Whole-mount immunostaining was carried out using the method of Faure et al. (2002) with an anti-phosphorylated SMAD1/5 antibody (1:100, Cell Signaling, 41D10, #9516). Peroxidase conjugated goat anti-rabbit IgG (1:300, Vector) was used as the secondary antibody. The fluorescent signal was developed using the tyramide signal amplification Plus system (PerkinElmer).

TUNEL-labeling of whole mount preparations was performed using a previously described method (Noro et al., 2011) except that proteinase K was used at 1 μg/ml for 15 min and the TUNEL reaction was performed using the In Situ Cell Death Detection Kit, TMR red (Roche). We counted TUNEL-positive nuclei in an area approximately $600 \times 600\ \mu m^2$ around the implanted bead and a similarly sized area on the contralateral side.

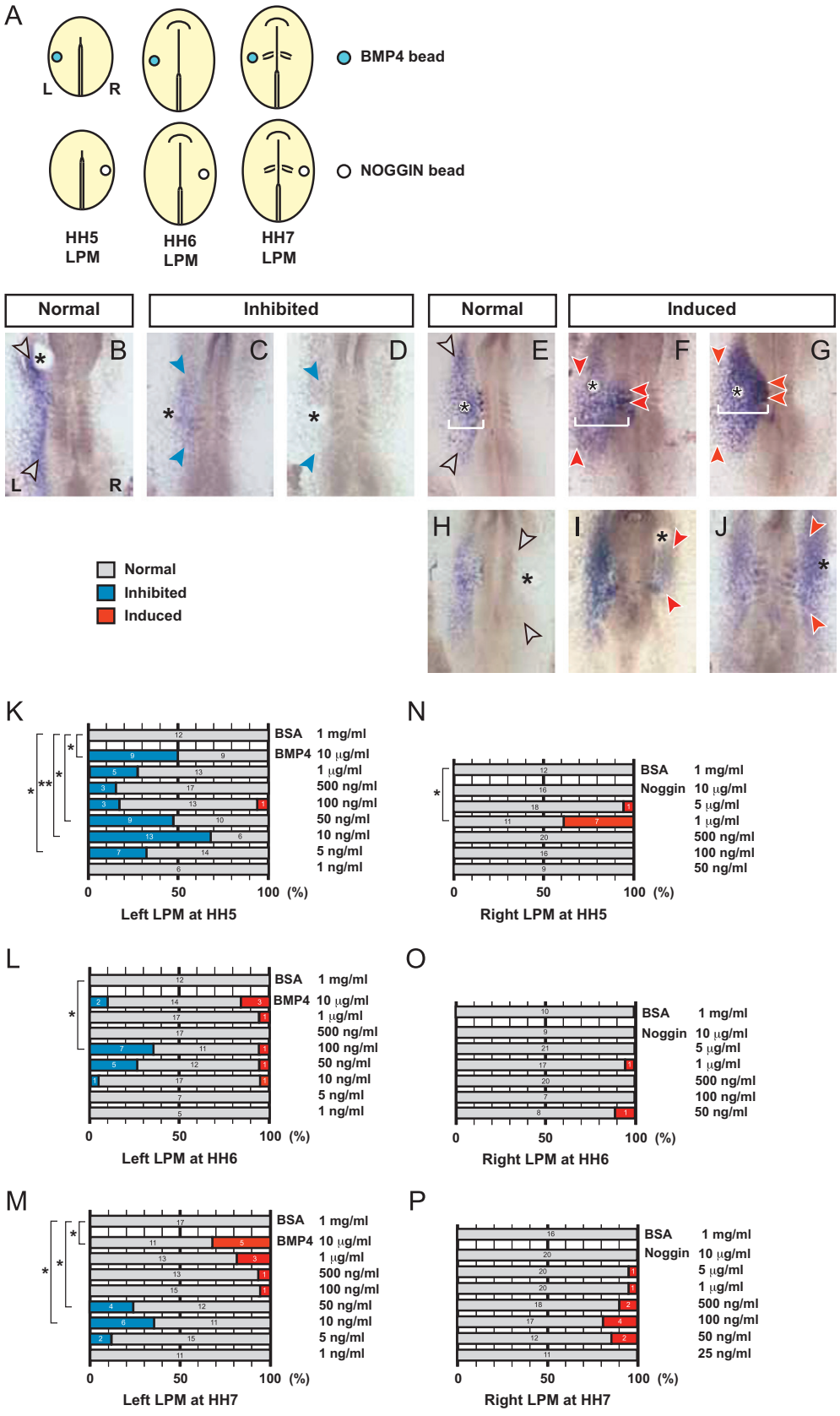

Fig. 1. Low concentration BMP4 inhibits and low concentration NOGGIN induces *Nodal* expression in the LPM: (A) BMP4 (1 ng/ml–10 μg/ml)-soaked beads (blue circles) were implanted into the left LPM and NOGGIN (25 ng/ml–10 μg/ml)-soaked beads (white circles) were implanted into the right LPM of chick embryos at the indicated developmental stages. *Nodal* expression was examined at HH8. L, left side; R, right side. (B–J) Examples of embryos showing inhibition or induction of *Nodal* expression. Embryos implanted with BMP4-soaked beads are shown in the upper panels and embryos implanted with NOGGIN-soaked beads are in the lower panels. Black asterisks show the positions of bead placement; gray arrowheads indicate the normal expression level of *Nodal*; blue arrowheads indicate inhibited *Nodal* expression; red arrowheads indicate induced *Nodal* expression; white bars show the width of the *Nodal* expression domain. (K–P) Stacked bar charts showing the percentages of phenotypes at each concentration in the implantation experiments. BMP4-beads (K–M) or NOGGIN-beads (N–P) were implanted into the LPM at HH5 (K and N), HH6 (L and O) and HH7 (M and P). The extent of *Nodal* expression was classified into three types: normal (gray), inhibited (blue), and induced (red). The numbers of embryos exhibiting each phenotype are shown on each bar. Asterisks indicate significant differences: $^{**}P < 0.01$; $^{*}P < 0.05$.

RT-PCR

Right lateral plate tissue (an area approximately 600 × 600 μm^2 around the implanted bead) was isolated from at least three embryos at HH8. RNA was isolated using ISOGEN II (NIPPON GENE) and cDNAs were synthesized using the Transcriptor High Fidelity cDNA Synthesizing Kit (Roche). The RT-PCR assay was performed as described by Nakayama et al. (2006) using PTC-200 (Bio-Rad). A 1 μl aliquot of the reverse transcription reaction mixture was used in a PCR reaction (20 μl) containing GoTaq Green Master Mix (Promega). The following PCR conditions were used: denaturation at 95 °C for 10 min, followed by 32–45 cycles of denaturation at 95 °C for 30 s, annealing at 55 °C for 30 s, and extension at 72 °C for 30 s. *GAPDH*, *Cfc*, and *Nodal* were amplified using 32, 34, and 45 PCR cycles, respectively. The following primers were used:

GAPDH, forward, 5′–ACGCCATCACTATCTTCCAG–3′, reverse, 5′–CAGCCTTCACTACCCTCTTG–3′; *Cfc*, forward, 5′–TCCGTGCCTGTCTTGGTACTGT–3′, reverse, 5′–AGTCGCCATGGATGATGCTG–3′; *Nodal*, forward, 5′–CCATGGCGTCCCTGTCTGGAAGCCAGGAGG–3′, reverse, 5′–GAGCTCTCCACTGCCCTGAGGAGGCTG–3′.

Surface plasmon resonance analyses

The binding experiments and analyses of kinetics were performed using the BIAcore 2000 system (GE Healthcare). Protein A (Nacalai Tesque, Japan) was immobilized on a CM5 sensor chip (GE Healthcare) by amine coupling to give a response of about 3300 response units. Chicken Caronte Fc chimera (R&D Systems) was captured on the sensor chip at about 2800 response units. Human BMP4, mouse NODAL and human Activin A (R&D Systems) were used as the analytes. Binding assays were performed in HBS-P buffer (10 mM Hepes (pH7.4), 150 mM NaCl, 0.005% Tween 20) at 25 °C and a flow rate of 20 ml/min. The data from the kinetic analyses were analyzed using BIAevaluation software version 4.1 (GE Healthcare).

Immunoblot analysis

To determine the level of phosphorylated Smad1, embryos were implanted with control or BMP4 (10 μg/ml) beads on the right LPM at HH5, HH6 or HH7. Right lateral plate tissue (an area approximately 600 × 600 μm^2 around the implanted bead) was isolated from three embryos at 120 min after implantation. Explants were homogenized in SDS sample buffer, subjected to SDS-PAGE and transferred to Clear-Blot membrane-P (ATTO). Proteins were detected using antibodies against Smad1 (1:1000, D59D7, #6944, Cell Signaling), Smad2 (1:2000, D43B4, #5339, Cell Signaling), phosphorylated-Smad1/5/8 (1:1000, #AB3848, Millipore), and actin (1:3000, A2066, Sigma), diluted in Signal Enhancer HIKARI (Nacalai Tesque, Japan). Protein bands were visualized using Immunostar-LD (Wako Pure Chemical Industries) and analyzed using an LAS-4000 Mini digital imager (GE Healthcare). Signal intensity was quantified using ImageJ 1.45s software (NIH). All data were expressed relative to actin.

Statistical analysis

The data were analyzed by Fisher's exact test or Student's *t*-test. $P < 0.05$ was considered statistically significant.

Results

Effect of different levels of BMP4 and NOGGIN on Nodal expression in the LPM

To test our hypothesis that the pattern of *Nodal* expression varies with the level of BMP signaling, we applied various concentrations of recombinant BMP4 or NOGGIN proteins to chick embryos at stages HH5 to HH7 of development and examined *Nodal* expression in the LPM at HH8. As previous studies have described the effects of high concentrations of BMP (0.1–1 mg/ml) and NOGGIN (0.2–2 mg/ml) (Monsoro-Burq and Le Douarin, 2001; Piedra and Ros, 2002; Yu et al., 2008), we used lower protein concentrations here, namely, 1 ng/ml–10 μg/ml BMP and 25 ng/ml–10 μg/ml NOGGIN.

First, we examined the effects of BMP4 on the left LPM as both up- and down-regulation of *Nodal* expression can be monitored in this tissue. Beads soaked in a BMP4 solution were implanted into the left LPM of chick embryos at HH5, in which *Nodal* expression is not detectable, at HH6, in which *Nodal* expression is initiated in the left-perinodal region, and at HH7, in which asymmetric expression of *Nodal* in the LPM is evident (Fig. 1A). Several patterns of *Nodal* expression were observed in the LPM and these were subjectively classified according to their appearance: "normal", essentially the same staining pattern as in untreated embryo (Fig. 1B, E and H); "inhibited", reduced expression in the left LPM (Fig. 1C) or no detectable expression in the left LPM (Fig. 1D); and "induced", weakly extended expression into the left paraxial mesoderm (Fig. 1F), weak expression in the right LPM (Fig. 1I), strongly extended expression into the left paraxial mesoderm (Fig. 1G) or approximately the same expression level in the right LPM as in the left LPM (Fig. 1J). The effect of the BMP4 treatment varied with concentration and embryonic stage: in HH5 embryos, BMP4 had an inhibitory effect at 5–50 ng/ml and 10 μg/ml (Fig. 1K); in HH6 embryos, BMP4 had an inhibitory effect at 100 ng/ml (Fig. 1L); in HH7 embryos, BMP4 had inhibitory effect at 10–50 ng/ml (Fig. 1M). However, BMP4 also induced *Nodal* expression in some embryos at HH7 (Fig. 1M). In these embryos, *Nodal* expression showed an expanded distribution in the LPM and was up-regulated in the paraxial mesoderm (Fig. 1F and G). The other concentrations tested had a significantly lower effect on *Nodal* expression. The rate of cell death did not differ significantly between embryos treated with 10 μg/ml BMP4 and control embryos (Supplementary Fig. S2), indicating that the change in *Nodal* expression was not caused by a reduction in the cell population in the LPM induced by a high concentration of BMP4. These results indicate that a low concentration of BMP4 (5–100 ng/ml) had an inhibitory effect on *Nodal* expression, whereas a high concentration (10 μg/ml) had either an inhibitory or inducing effect depending on the embryonic stage of implantation.

Next, we examined the effects of different concentrations of NOGGIN. We applied NOGGIN to the right LPM because ectopic *Nodal* expression is more easily monitored in this side of the embryo. We found that HH5 embryos showed induction of *Nodal* expression when treated with 1 μg/ml NOGGIN (Fig. 1N). Concentrations of NOGGIN above or below 1 μg/ml had no apparent effect on *Nodal* expression. Application of NOGGIN at HH6 and HH7 resulted in a lower rate of induced *Nodal* expression compared to HH5 (Fig. 1N–P). The results presented here indicate that BMP signaling has distinct roles depending on concentration and embryonic stage. Between HH5 and HH7, a low concentration of BMP4 inhibits *Nodal* expression in the LPM, while a low concentration of NOGGIN induces its expression; at HH7, however, a high concentration of BMP4 induces *Nodal* expression in the LPM. These observations indicate both a negative and positive role for BMP signaling on *Nodal* expression.

The results shown in Fig. 1 and from previous studies (Piedra and Ros, 2002; Schlange et al., 2002; Yu et al., 2008) strongly suggest that BMP signaling has multiple effects on *Nodal* expression in the LPM. To investigate this possibility further, we applied BMP and NOGGIN to the right LPM and subsequently sampled the tissues to screen for *Nodal* expression (Fig. 2). *Bmp2*, *4* and *7* are expressed in the LPM between HH4 and HH7 (Monsoro-Burq and Le Douarin, 2000; Yokouchi et al., 1999). To eliminate endogenous BMP signaling in the LPM, NOGGIN (1000 μg/ml) was added to the solutions in which the beads were soaked. This concentration is sufficient to suppress *Cfc*, which is both a co-receptor for NODAL and a BMP dependent gene in the LPM (Piedra and Ros, 2002; Schlange et al., 2001). Beads soaked in a range of BMP4 solutions (5–1000 μg/ml) containing NOGGIN (1000 μg/ml) were implanted into the right LPM at HH5. The right lateral plate tissues around the beads were isolated from the embryos at HH8, and *Nodal* expression in the isolated tissues was examined by RT-PCR (Fig. 2A). Ectopic *Nodal* induction was found after treatment with 50 μg/ml BMP4 but not at the other concentrations used (Fig. 2B). As expected, *Cfc* expression was dependent on BMP in the LPM. Expression of *Cfc* was suppressed by 1000 μg/ml NOGGIN but gradually increased as the concentration of BMP4 increased (Fig. 2B). We also confirmed that *Nodal* was up-regulated by 1000 μg/ml BMP4 applied at HH7 as reported by Piedra and Ros (2002).

From the results of the two experiments described above, we conclude that *Nodal* expression in the LPM is regulated differentially by four levels of BMP signaling. We label these levels here as low, low intermediate, high intermediate, and high. The low intermediate and high levels of BMP signaling are sufficient for *Nodal* expression in the LPM. The low intermediate level (50 μg/ml BMP4 plus 1000 μg/ml NOGGIN) provided an optimal level of BMP signaling for *Nodal* expression in the LPM; this effect was also seen after application of low concentrations of NOGGIN to the right LPM (Fig. 1F).

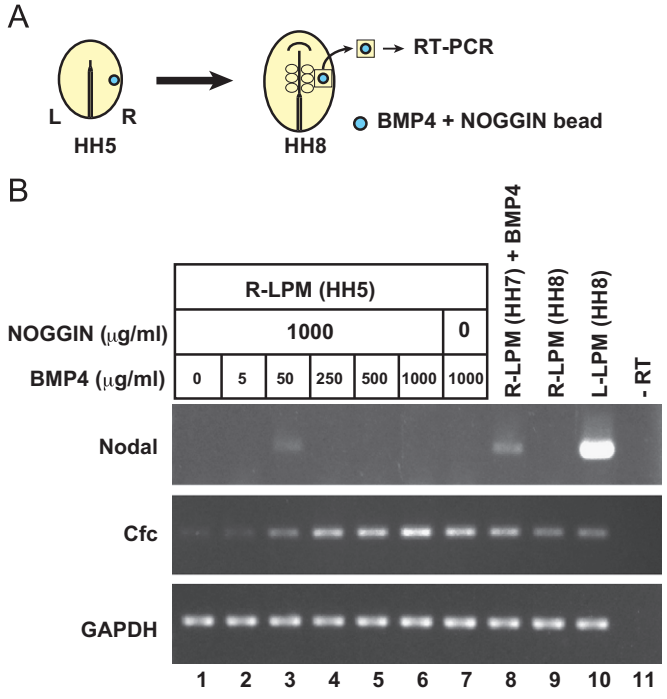

Fig. 2. Expression profile of *Nodal* in the right LPM following treatment with different concentrations of BMP4. Beads were soaked in a range of BMP4 concentrations in the presence of NOGGIN and then implanted into the right LPM at HH5. The regions around the implantation sites were dissected out at HH8 and processed for RT-PCR. (B) RT-PCR analysis of *Nodal*, *Cfc*, and *GAPDH* expression. Lanes 1–6: R-LPMs treated with 5, 50, 250, 500 or 1000 μg/ml BMP4 in the presence of NOGGIN (1000 μg/ml). *Nodal* expression was detected only at the 50 μg/ml BMP4 dose. In contrast, *Cfc* expression showed increasing up-regulation with increasing BMP4 concentration. Lane 7: R-LPMs implanted at HH5 with beads soaked in 1000 μg/ml BMP4. Lane 8: R-LPMs implanted at HH7 with beads soaked in 1000 μg/ml BMP4. Lane 9: R-LPMs from untreated HH8 embryos. Lane 10: L-LPM from untreated HH8 embryos. Lane 11: RT-PCR of L-LPM from HH8 embryos in the absence of reverse transcriptase.

Manipulation of BMP signaling during early developmental stages affects *Shh* expression in the node; high concentrations of BMP applied to the embryo between HH4 and HH6 suppress *Shh* expression in the node, leading to abolition of *Nodal* expression in the LPM. By contrast, high concentrations of NOGGIN induce *Shh* expression in the node (Monsoro-Burq and Le Douarin, 2001; Piedra and Ros, 2002). We tested whether low concentrations of BMP4 and NOGGIN affect *Shh* expression in the node. Beads soaked in 10 ng/ml BMP4 or 1 μg/ml NOGGIN (the most effective doses for affecting *Nodal* expression when implanted at HH5; Fig. 1K and N) were applied to the LPM or perinodal region and *Shh* expression was examined at HH6 (Supplementary Fig. S2). The concentrations of BMP4 and NOGGIN used here had no effect on *Shh* expression (Supplementary Fig. S2). Thus, the slight changes in the BMP signaling level resulting from low concentrations of BMP4 and NOGGIN can affect *Nodal* expression in the LPM without disturbing *Shh* expression in the node.

The induction of Nodal by a low concentration of NOGGIN depends on NODAL receptor signaling

The results shown in Fig. 1 suggest that asymmetric BMP signaling in the left and right LPMs might occur during early developmental stages in the chick embryo. We investigated BMP signaling activities during the early stages of L–R axis formation using immunostaining with an anti-phosphorylated SMAD1/5 antibody. Phosphorylated SMAD1/5 (pSMAD1) was found to be uniformly distributed on both sides of the LPM of the chick embryo from HH5 to HH8 (Supplementary Fig. S3). These results indicate that BMP signaling activity is equal on each side of the LPM in the chick embryo.

We then examined changes in BMP signaling activity in the LPM of embryos implanted with BMP- or NOGGIN-soaked beads (Supplementary Fig. S4). The selected concentrations of BMP4 and NOGGIN were those found to be most effective at influencing *Nodal* expression in the earlier experiment (Fig. 1): BMP4, 10 μg/ml and 10 ng/ml (HH5 and HH7), and 100 ng/ml (HH6); NOGGIN, 1 μg/ml (HH5). The regions around the implantation sites were dissected out 120 min after implantation and processed for immunoblotting using anti-phosphorylated SMAD1. No significant differences to controls were found in embryos implanted with BMP4 at 10 ng/ml or NOGGIN at 1 μg/ml (Supplementary Fig. S4), although these treatments were effective at inhibiting or inducing *Nodal* expression, respectively.

We next sought to determine how an equal level of BMP signaling could produce differences in *Nodal* expression on each side of the LPM. Recent reports have shown that BMP and ACTIVIN/NODAL signaling pathways antagonize each other through competition between SMAD1 and SMAD2 for their binding to the common component SMAD4 (Candia et al., 1997; Furtado et al., 2008; Yamamoto et al., 2009). In addition, NODAL up-regulates its expression by a positive feedback loop (Hamada et al., 2002). On the basis of these observations, we hypothesized that a low concentration of NOGGIN might act synergistically with NODAL to increase *Nodal* expression from the background level by activating a NODAL positive-feedback loop. To test this hypothesis, we first examined whether *Nodal* induction by a low concentration of NOGGIN depended on NODAL receptor signaling. NOGGIN-soaked beads were implanted into the right LPM at HH5

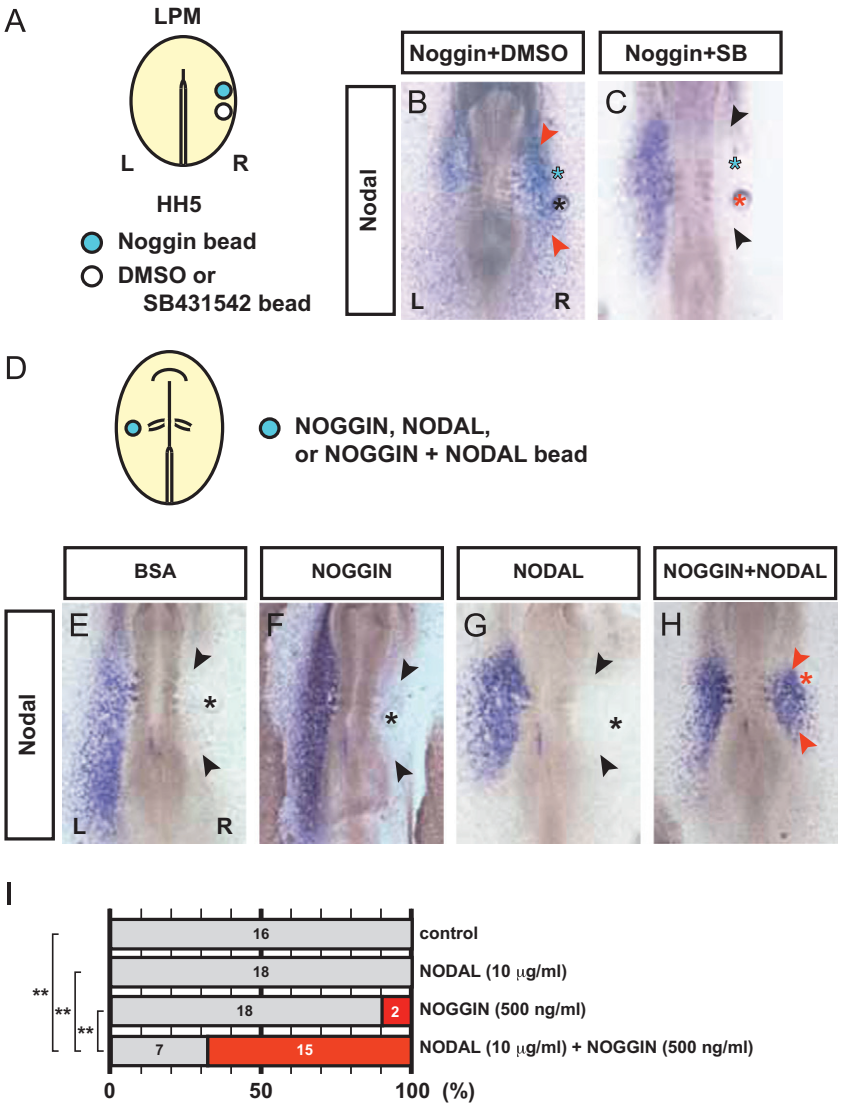

Fig. 3. *Nodal* induction by low concentration NOGGIN depends on a NODAL positive feedback loop: (A) beads soaked in a low concentration (1 μg/ml) of NOGGIN were implanted together with beads soaked in SB431542 into the right LPM at HH5, and *Nodal* expression was examined at HH8. (B) Control DMSO beads (black asterisk) had no effect on *Nodal* induction by NOGGIN (green asterisk), resulting in ectopic *Nodal* induction (red arrowheads). (C) SB431542 (10 mM, red asterisk) completely suppressed ectopic *Nodal* induction (black arrowheads) by NOGGIN (green asterisk). (D–I) Low concentrations of NOGGIN and NODAL synergistically induce *Nodal* expression. (D) Beads soaked in NODAL (10 μg/ml), NOGGIN (500 ng/ml), or NODAL (10 μg/ml) plus NOGGIN (500 ng/ml) were implanted into the right LPM at HH7. Control BSA, NODAL alone, and NOGGIN alone (E–G, black asterisks) did not induce *Nodal* expression (black arrowheads), whereas NODAL plus NOGGIN (red asterisk) effectively induced *Nodal* expression (H, red arrowheads). (I) Bar chart summary of the results showing the percentages of each phenotype. The extent of *Nodal* expression was classified as shown in Fig. 1. Asterisks indicate significant differences in ectopic *Nodal* induction: **, $P < 0.01$.

together with beads soaked either in SB431542, an inhibitor of the ACTIVIN/NODAL receptor, or in DMSO (Fig. 3A). NOGGIN (1 μg/ml) with DMSO induced *Nodal* in the right LPM in 3 of 6 embryos (50%, Fig. 3B). In contrast, SB431542 completely suppressed *Nodal* induction by NOGGIN (Fig. 3C, $n=6$). Thus, *Nodal* induction by 1 μg/ml NOGGIN depends on NODAL receptor signaling. This result suggests that NODAL and low concentration NOGGIN act synergistically to induce *Nodal* expression. Therefore, we examined the synergy between NOGGIN and NODAL. Beads that had been soaked in 10 μg/ml NODAL did not induce *Nodal* when implanted into the right LPM at HH7 (Fig. 3 G, I; $n=18$). In the first experiment described here (Fig. 1H), beads soaked in 500 ng/ml NOGGIN did not significantly induce *Nodal* when implanted into the right LPM at HH7; only weak induction was observed in 2 of 20 embryos (10%). However, when beads soaked in 10 μg/ml NODAL plus 500 ng/ml NOGGIN were implanted into the right LPM at HH7, *Nodal* was induced in 15 of 22 embryos (68%, Fig. 3H, I). We conclude that NODAL and low concentration NOGGIN act synergistically to induce *Nodal* expression in the LPM. Additionally, our results indicate that NOGGIN is an effective inducer of *Nodal* even at HH7 if the appropriate amount of NODAL is available in the right LPM.

BMP signaling and NODAL signaling compete for SMAD4 in the LPM

Next, we examined whether BMP signaling and NODAL signaling compete in the chick embryo. In order to introduce a directly activated BMP or NODAL signal, we electroporated an expression vector carrying a constitutively active form of the BMP receptor (pc3-*caAlk6*) or a constitutively active form of the ACTIVIN/NODAL receptor (pc3-*caAlk4*) into chick embryos. Chick embryos received either one or both vectors into the middle primitive streak region of the epiblast (the prospective LPM) at HH4 (Fig. 4A); cells from this region migrate to the LPM without being

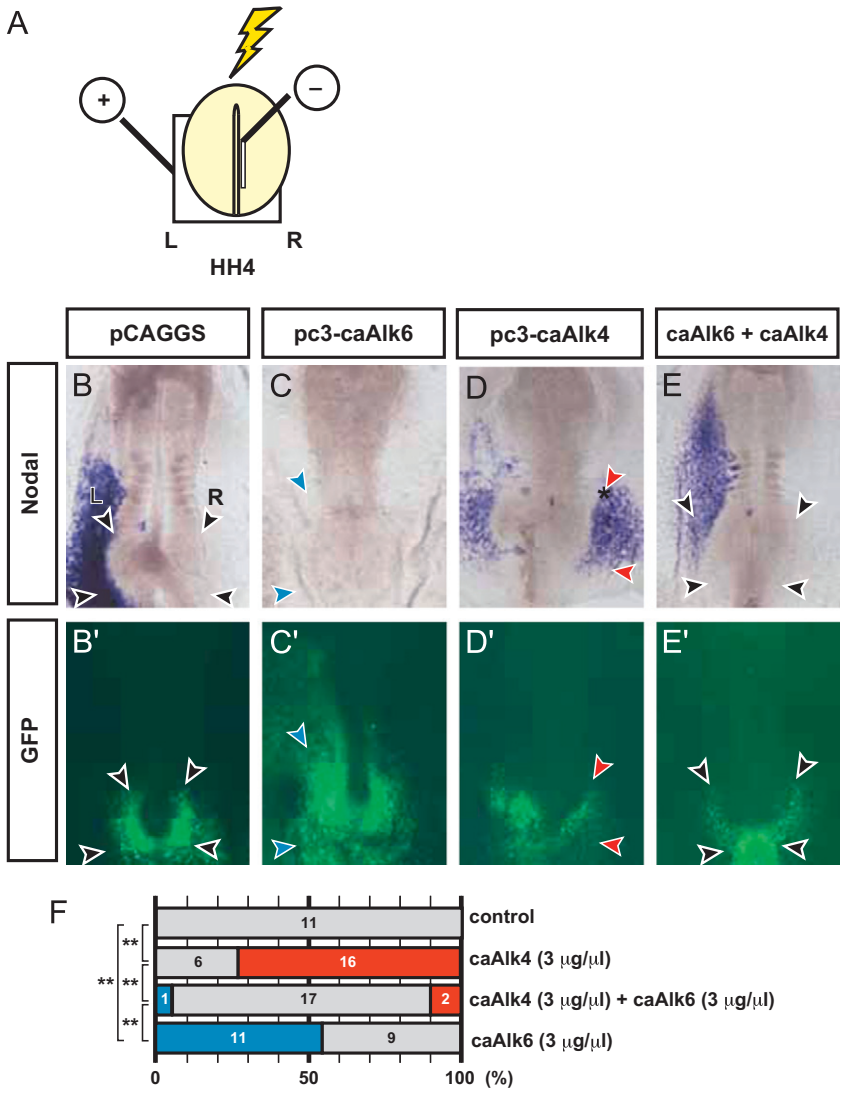

Fig. 4. BMP signaling and NODAL signaling mutually suppress their effects on *Nodal* expression in the LPM (A) pc3-*caALK4*, pc3-*caALK6*, or pCAGGS (control) with pCAGGS-*GFP* were electroporated into the middle primitive streak region of the epiblast at HH4 and *Nodal* expression was examined at HH8. (B and B′) No effect on *Nodal* expression in the LPM was seen in the control (black arrowheads). (C and C′) *caALK6* repressed endogenous *Nodal* expression in the left LPM (blue arrowheads). (D and D′) *caALK4* induced ectopic *Nodal* expression in the right LPM (red arrowheads). (E and E′) Co-introduction of *caALK6* and *caALK4* resulted in a mutual suppression of their effects on *Nodal* expression in the LPM (black arrowheads). (F) Bar chart summary of the results showing percentages of each phenotype. The extent of *Nodal* expression was classified as shown in Fig. 1. Asterisks indicate significant differences in *Nodal* inhibition (between control and caAlk6, and between caAlk4+caAlk6 and caAlk6) or ectopic *Nodal* induction (between control and caAlk4, and between caAlk4+caAlk6 and caAlk4); $^{**}P<0.01$.

incorporated into the node (Psychoyos and Stern, 1996; Yang et al., 2002). *Nodal* expression was then examined at HH8. Electroporation of 3 μg/μl pc3-*caAlk6* suppressed *Nodal* expression in the left LPM in 11 of 20 embryos (55%, Fig. 4C, C′ and F). This outcome is similar to that seen in this study for a low intermediate level of BMP signaling. In contrast, 3 μg/μl pc3-*caAlk4* induced *Nodal* expression in the right LPM in 16 of 22 embryos (73%, Fig. 4D, D′ and F). When both constructs (each at 3 μg/μl) were introduced, *Nodal* suppression in the left LPM was found in only 1 of 20 embryos (5%, Fig. 4F) and *Nodal* induction in the right LPM was found in only 2 of 20 embryos (10%, Fig. 4F). The normal left-sided expression of *Nodal* was present in 17 of 20 embryos (85%, Fig. 4E, E′ and F). The control pCAGGS had no effect on *Nodal* expression ($n=11$, Fig. 4B, B′ and F). These results indicate that BMP signaling and NODAL signaling inhibit each other in a dose dependent manner.

One possible explanation for the antagonistic behavior of BMP and ACTIVIN/NODAL signaling is competition between SMAD1 and SMAD2 for the limiting amounts of the common factor SMAD4 (Furtado et al., 2008). The BMP signaling pathway has been shown to inhibit the ACTIVIN/NODAL signaling pathway in vitro, and overexpression of *Smad4* reverses this inhibition (Candia et al., 1997; Furtado et al., 2008). In the mouse embryo, BMP signaling activity is higher in the right LPM (Mine et al., 2008); expression of *Pitx2*, a downstream target of NODAL signaling, is normally absent in the right LPM, however, overexpression of *Smad4* in the right LPM up-regulates *Pitx2* expression (Furtado et al., 2008). From these data, we hypothesized that if competition between BMP signaling and NODAL signaling regulates *Nodal* expression in the LPM of the chick embryo, overexpression of *Smad4* in the right LPM could activate *Nodal* expression. To test this possibility, pCAGGS-*Smad4* was electroporated into the prospective LPM. Overexpression of *Smad4* in the right LPM induced *Nodal* expression in 14 of 25 embryos (56%, Fig. 5C, C′and F) while introduction of a control vector had no effect ($n=13$, Fig. 5B, B′and F). To test whether *Nodal* induction by

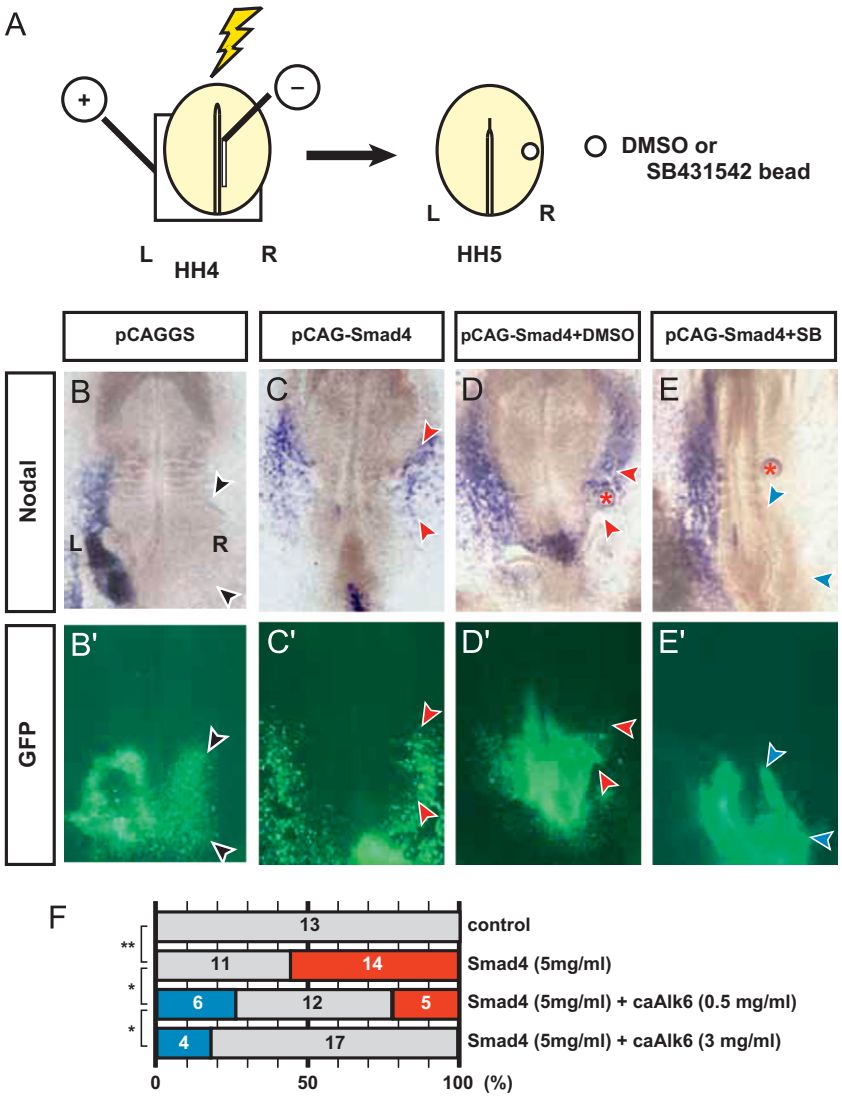

Fig. 5. Effects of *Smad4* overexpression on *Nodal* expression in the LPM: (A) pCAGGS-*Smad4* or pCAGGS (control) along with pCAGGS-*GFP* were electroporated into the middle primitive streak region of the epiblast at HH4 and *Nodal* expression was examined at HH8. (B and B′) The control embryo showed no effect on *Nodal* expression in the LPM (black arrowheads). (C and C′) *Smad4* induced ectopic *Nodal* expression in the right LPM (red arrowheads). (D and E′) Beads soaked in DMSO or SB431542 were implanted at HH5 following electroporation of pCAGGS-*Smad4* at HH4. Control DMSO beads (black asterisk) had no effect on *Nodal* induction by *Smad4* overexpression, resulting in bilateral *Nodal* expression (red arrowheads) (D and D′). SB431542 (10 mM, red asterisk) completely suppressed ectopic *Nodal* induction by *Smad4* overexpression (blue arrowheads) (E and E′). (F) BMP signaling suppressed ectopic *Nodal* induction by SMAD4. pCAGGS-*Smad4* and pc3-*caAlk6* were introduced together at the indicated concentrations. The frequency of ectopic *Nodal* induction in the right LPM decreased as the concentration of pc3-*caAlk6* increased. The extent of *Nodal* expression was classified as shown in Fig. 1. Asterisks indicate significant differences in ectopic *Nodal* induction: $^{**}P<0.01$; $^{*}P<0.05$.

Smad4 overexpression depended on NODAL receptor signaling, embryos that had been induced to overexpress *Smad4* were implanted with beads soaked in SB431542 or DMSO into the right LPM at HH5 (Fig. 5A). SB431542 suppressed the induction of *Nodal* by *Smad4* overexpression in 22 of 23 embryos (96%, Fig. 5E and E′) while control DMSO did not affect the frequency of *Nodal* induction by *Smad4*; ectopic *Nodal* induction was found in 17 of 29 embryos (59%, Fig. 5D and D′). These results indicate that *Nodal* induction by *Smad4* overexpression depends on NODAL receptor signaling.

To test whether BMP signaling and ACTIVIN/NODAL signaling compete for SMAD4, we co-electroporated pCAGGS-*Smad4* and pc3-*caAlk6* into chick embryos. The introduction of 5 μg/μl pCAGGS-Smad4 and 0.5 μg/μl pc3-*caAlk6* resulted in ectopic *Nodal* induction in the right LPM in only 5 of 23 embryos (22%, Fig. 5F). One embryo showed strong inhibition of endogenous *Nodal* expression (4%, Fig. 5F). Introduction of 5 μg/μl pCAGGS-*Smad4* and 3 μg/μl pc3-*caAlk6* resulted in none of the embryos showing ectopic *Nodal* induction, whereas normal left-sided expression of *Nodal* was observed in 17 of 21 embryos (81%, Fig. 5F). Four embryos showed weak inhibition of endogenous *Nodal* expression (19%, Fig. 5F). These results indicate that activation of BMP signaling reversed the induction of *Nodal* due to *Smad4* overexpression and did so in a dose dependent manner. Overexpression of *Smad4* did not affect *Cfc* expression (control, $n=13$; Smad4, $n=9$; Supplementary Fig. S5), suggesting that the amount of exogenously added *Smad4* was insufficient to cause strong activation of BMP signaling. Overall, our results indicate that overexpression of *Smad4* in the right LPM activates a NODAL positive feedback loop, and suggest that BMP signaling and NODAL signaling compete for SMAD4 in the LPM of the chick embryo.

Low SMAD1 level up-regulates Nodal expression in the LPM but low SMAD2 level downregulates expression

If competition between BMP and NODAL signaling regulates *Nodal* expression in the LPM, then down-regulation of SMAD1 or SMAD2 should shift the balance of the SMAD complexes and lead to a perturbation of *Nodal* expression in the LPM. To test this hypothesis, we used morpholino oligonucleotides (MOs) to knock-down SMAD1 or SMAD2 in chick embryos. An immunoblotting analysis showed that the Smad1 and Smad2 MOs reduced production of their target protein to approximately one-third of the control level (Supplementary Fig. S6). A control, Smad1 or Smad2 MO was electroporated into the prospective LPM at HH4 and *Nodal* expression was examined at HH8 (Fig. 6). Smad1 MO induced *Nodal* expression in the right LPM in 8 of 22 embryos (36%, Fig. 6C, C′ and E). In contrast, Smad2 MO suppressed *Nodal* expression in the left LPM in 9 of 20 embryos (45%, Fig. 6D, D′ and E). The control MO had no effect on *Nodal* expression ($n=15$, Fig. 6B, B′ and E). These data are consistent with the expectation that changes in the balance of SMAD complexes as a result of down-regulation of SMAD1 or SMAD2 can cause altered *Nodal* expression. The experiment therefore provides support for our suggestion that competition between BMP and NODAL signaling regulates *Nodal* expression in the LPM.

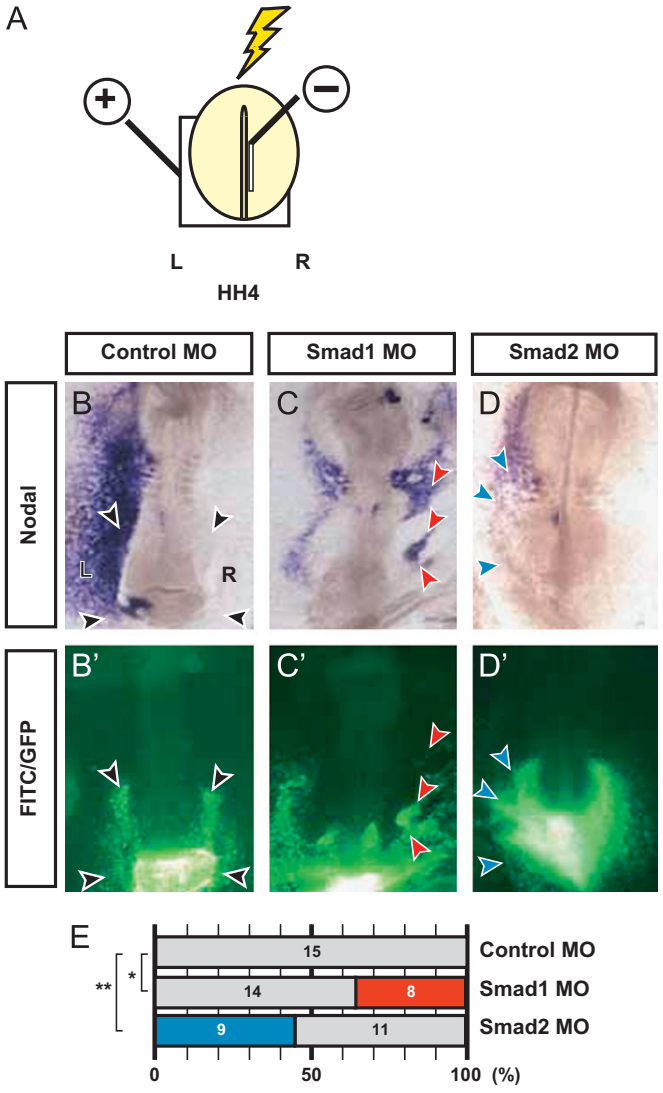

Fig. 6. BMP signaling and NODAL signaling mutually suppress their effects on *Nodal* expression in the LPM (A) Control MO, Smad1 MO, or Smad2 MO were electroporated into the middle primitive streak region of the epiblast at HH4 and *Nodal* expression was examined at HH8. (B and B′) No effect on *Nodal* expression in the LPM was seen in the control MO (black arrowheads). (C and C′) Smad1 MO induced ectopic *Nodal* expression in the right LPM (red arrowheads). (D and D′) Smad2 MO repressed endogenous *Nodal* expression in the left LPM (blue arrowheads). (E) Bar chart summary of the results showing percentages of each phenotype. The extent of *Nodal* expression was classified as shown in Fig. 1. Asterisks indicate significant differences in ectopic *Nodal* induction (between control and Smad1 MO) or *Nodal* inhibition (between control and Smad2 MO): $^{**}P<0.01$; $^{*}P<0.05$.

Activation of Nodal expression by a High concentration of BMP4 depends on Cfc up-regulation and NODAL receptor signaling

We also investigated the possibility that a high concentration of BMP can up-regulate *Nodal* expression (Piedra and Ros, 2002; Yu et al., 2008). Previous studies indicated that *Nodal* induction by a high concentration of BMP might be an indirect effect that acts via up-regulation of *Cfc*, a co-receptor for the NODAL receptor; this up-regulation of *Cfc* then sensitizes the cells to NODAL (Piedra and Ros, 2002; Schlange et al., 2002). To assess this possibility, we first investigated whether *Nodal* induction by a high concentration of BMP4 depended on NODAL signaling. Beads were soaked in 100 μg/ml BMP4, a concentration that up-regulates both *Nodal* and *Cfc* expression in the LPM (Piedra and Ros, 2002), and then implanted into the right LPM at HH7 together with SB431542-beads or DMSO-beads as controls (Fig. 7A). BMP4 plus DMSO was found to induce *Nodal* in the right LPM in 9 of 10 embryos (90%, Fig. 7B). In contrast, BMP4 with SB431542 suppressed *Nodal* induction by BMP4 in all embryos ($n=10$, Fig. 7C). These results confirm that *Nodal* induction by high concentration BMP is an indirect effect and depends on NODAL receptor signaling.

We next investigated whether *Cfc* overexpression leads to *Nodal* induction. To test this, pCAGGS-*Cfc* was electroporated into the prospective LPM at HH4. Overexpression of *Cfc* in the right LPM induced *Nodal* expression in 9 of 18 embryos (50%, Fig. 7E and E′) whereas the control had no effect ($n=11$, Fig. 7D and D′). These results are consistent with those for the *Xenopus Cfc* orthologue, *XCR2* (Onuma et al., 2006), and indicate that *Cfc* overexpression is sufficient for *Nodal* induction. To test whether *Nodal* induction by *Cfc* overexpression depended on NODAL signaling, SB431542-beads were implanted following electroporation of pCAGGS-*Cfc*. SB431542 completely suppressed the induction of *Nodal* mediated by *Cfc* overexpression ($n=7$, Fig. 7G and G′), whereas the DMSO control had no effect and ectopic *Nodal* induction was found in 5 of 12 embryos (42%, Fig. 7F and F′). These results suggest that *Nodal* induction by *Cfc* overexpression also depends on NODAL receptor signaling. Taken together, our observations support the proposal that a high concentration of BMP activates *Nodal* expression via up-regulation of *Cfc* expression (Piedra and Ros, 2002; Schlange et al., 2002).

In light of the evidence that the level of expression of *Cfc* affects *Nodal* expression, we investigated whether the pattern of *Cfc* expression is altered after application of a low concentration of BMP4 or NOGGIN. We found that application of BMP4 (10 or 100 ng/ml) or NOGGIN (1 μg/ml) into the LPM had no effect on *Cfc* expression in the LPM (Supplementary Fig. S1). Thus, the mechanism of *Nodal* regulation by low concentrations of BMP4 and NOGGIN is independent of changes in *Cfc* expression and, therefore, differs from the mechanism activated by high concentrations of BMP and NOGGIN.

Binding responses of CARONTE to BMP4 and NODAL

Next, we investigated the possible role of CERBERUS/CARONTE, which is a candidate molecule for inhibiting BMP signaling

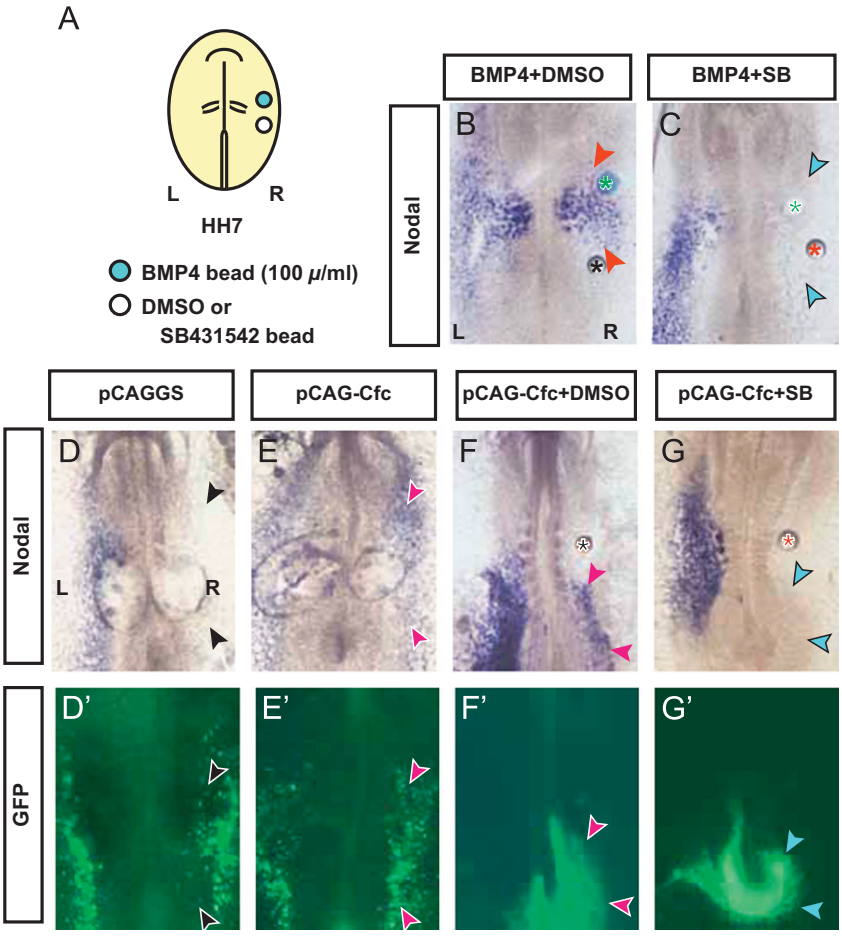

Fig. 7. Mechanism of *Nodal* induction by a high concentration of BMP4: (A) beads that had been soaked in a high concentration (100 μg/ml) of BMP4 were implanted (blue asterisk) together with beads soaked in SB431542 into the right LPM at HH7. (B) Control DMSO beads (black asterisk) had no effect on *Nodal* induction by BMP4, resulting in ectopic *Nodal* expression in the right LPM (red arrowheads). (C) SB431542 (red asterisk) completely suppressed ectopic *Nodal* induction (blue arrowheads) by BMP4 (green asterisk). (D and E) pCAGGS-*Cfc*, or pCAGGS (control) along with pCAGGS-*GFP* were electroporated into the middle primitive streak region of the epiblast at HH4 and *Nodal* expression was examined at HH8. (D and D′) Control pCAGGS had no effect on *Nodal* expression in the LPM (black arrowheads). (E and E′) *Cfc* induced ectopic *Nodal* expression in the right LPM (red arrowheads). (F and G) *Nodal* induction by *Cfc* overexpression depended on NODAL signaling. Beads soaked in DMSO or SB431542 were implanted after electroporation. (F and F′) Control DMSO beads (black asterisk) had no effect on *Nodal* induction by *Cfc* overexpression, resulting in ectopic *Nodal* expression (red arrowheads). (G and G′) SB431542 (red asterisk) completely suppressed ectopic *Nodal* induction (blue arrowheads) by *Cfc* overexpression.

in the left LPM. CARONTE is a potent BMP antagonist that is expressed in the left paraxial mesoderm and left LPM from HH6 to HH8 (Rodriguez Esteban et al., 1999; Yokouchi et al., 1999; Zhu et al., 1999). Since it has been recently reported to function as a NODAL antagonist (Tavares et al., 2007), we performed a surface plasmon resonance analysis to compare the affinities of CARONTE to BMP and NODAL (Supplementary Fig. S7). As expected from previous reports (Rodriguez Esteban et al., 1999), CARONTE was found to bind to BMP4 and NODAL. CARONTE exhibited increased binding response as the concentration of BMP4 and NODAL increased, but did not show this response to the control protein ACTIVIN A (Supplementary Fig. S7). Therefore, we conclude that CARONTE binds to BMP4 and NODAL but not to ACTIVIN A. The apparent dissociation constants (K_D) for BMP4 and NODAL binding were calculated to be $1.9 \pm 0.5 \times 10^{-9}$ M and $2.8 \pm 1.3 \times 10^{-10}$ M, respectively, indicating that affinity between CARONTE and NODAL is slightly higher than between CARONTE and BMP4. In addition, kinetic analyses revealed that the association and dissociation rate constants for BMP4 were higher than those for NODAL (Supplementary Table S1), indicating that binding and dissociation between CARONTE and BMP4 is faster than between CARONTE and NODAL. These results suggest that when CARONTE, BMP4 and NODAL are present at the same time and at the same concentration, CARONTE might dynamically change its binding partner from BMP4 to NODAL.

Discussion

BMP signaling has multiple effects on Nodal expression in the LPM

BMP signaling was found to have a positive effect on the induction of *Nodal* expression after implantation of high concentrations of BMP and NOGGIN (Piedra and Ros, 2002; Yu et al., 2008). However, in experiments using implantation of cell pellets expressing growth factors, Yokouchi et al. (1999) found that BMP signaling had a negative role. These contrasting outcomes might reflect the different levels of growth factor used in the respective experiments. Since BMP is a known morphogen, it is possible that different concentrations might induce distinct responses in the LPM cells. We examined this possibility using a wide range of BMP and NOGGIN concentrations. Our experiments showed that specific concentrations of BMP4 applied to the left LPM at HH5 inhibited *Nodal* expression (Fig. 1K–M), whereas, NOGGIN applied to the right LPM at HH5 induced expression (Fig. 1N). We

conclude that different levels of BMP signaling differentially regulate *Nodal* expression in the LPM; we classified these levels as low, low intermediate, high intermediate, and high.

Only a small proportion of the embryos showed changes in *Nodal* expression after implantation of a bead (Fig. 1C–H). One possible explanation for this low rate is that the degree of contact between the bead and tissues differed among embryos. Following implantation, in some embryos the beads appeared to soak up water from the agar medium during incubation. Possibly, the water weakened the contact between the bead and the embryo and, thereby, lessened the effect of the BMP4 or NOGGIN.

The optimal concentration of BMP4 for inhibition of *Nodal* expression varied among embryonic stages (Fig. 1K–M). The concentration of BMP4 required for *Nodal* inhibition at HH6 was 10 times as high as those at HH5 and 7. This increase might be explained by the presence of an endogenous BMP antagonist at its peak level in the left LPM at HH6; the presence of this putative antagonist might lead to a requirement for a higher concentration of BMP4 to inhibit *Nodal* expression at HH6. We showed that NOGGIN was only effective at inducing *Nodal* at HH5 (Fig. 1N–P), that is, before the onset of asymmetric *Nodal* expression. The efficiency of NOGGIN-induced expression of *Nodal* was lower at HH6 and 7, when asymmetric *Nodal* expression is apparent. This decrease in induction potential might be explained by the availability of NODAL after HH6. As NODAL induces the negative regulators LEFTY-1 and CERBERUS/CARONTE in the chick embryo (Tavares et al., 2007), then only a small amount of NODAL might be available outside the left LPM after HH6. In agreement with this idea is the observation that NOGGIN can effectively induce *Nodal* even at HH7 when a sub-threshold, but appropriate, amount of NODAL is available in the right LPM (Fig. 3D–I). We also showed that 1 μg/ml NOGGIN was the optimal concentration for *Nodal* induction at HH5 and that higher and lower concentrations were not effective (Fig. 1N). These findings can be explained by the fact that higher concentrations of NOGGIN down-regulate *Cfc*, a co-receptor for NODAL (Piedra and Ros, 2002), whereas lower concentrations are insufficient to attenuate BMP signaling for *Nodal* induction.

Which molecule might be responsible for inhibiting BMP signaling in the left LPM from HH5 to HH7? One possible candidate for a BMP antagonist is CERBERUS/CARONTE although this protein has recently been reported to function as a NODAL antagonist (Tavares et al., 2007). We showed here that the affinity of CARONTE for NODAL is slightly higher than that of CARONTE for BMP4; moreover, the association and dissociation rate constants for BMP4 were higher than for NODAL (Supplementary Table S1). These results indicate that binding and dissociation of CARONTE and BMP4 is more rapid than of CARONTE and NODAL. We therefore propose that when CARONTE, BMP4 and NODAL are present at the same time and at the same concentration, CARONTE can dynamically change its binding partner from BMP4 to NODAL. Recent studies have suggested that pattern formation by NODAL and its inhibitor LEFTY follows a reaction–diffusion model (Shen, 2007; Shiratori and Hamada, 2006). According to this model, LEFTY diffuses faster than NODAL (Muller et al., 2012). Therefore, based on our kinetic data between CARONTE and BMP/NODAL, we propose following model for regulation of BMP and NODAL signaling by CARONTE. Assuming that L–R patterning by NODAL and CARONTE also fits a reaction–diffusion model, CARONTE is expected to diffuse faster than NODAL from the paraxial mesoderm to the LPM where BMPs, but not NODAL, are already present. As a result, CARONTE binds and inhibits BMPs until NODAL reaches the LPM. Once NODAL diffuses into the LPM and robust *Nodal* expression is activated, CARONTE switches its binding partner from BMPs to NODAL and acts as a NODAL inhibitor. As the relative diffusion rates of chicken NODAL and CARONTE have not yet been determined, this model will need to be assessed in a future study.

A second candidate for a binding factor is chicken DAN, which is a BMP antagonist that is expressed in the left side of the node from HH5 to HH7. However, it has not yet been determined whether DAN acts locally or at a distance in the LPM (Katsu et al., 2012). Overall, therefore, although we have provided evidence of a possible mechanism involving CARONTE, it is not possible to exclude the possibility of other factors being involved. Further studies will clearly be necessary to unambiguously elucidate the identities of BMP antagonists responsible for inhibiting BMP signaling in the left LPM.

Competition between BMP and NODAL signaling for SMAD4 regulates Nodal expression in the LPM

In the mouse embryo, *Noggin* and *Chordin* are expressed in the left LPM and suppress BMP signaling, resulting in an asymmetric distribution of pSMAD1 in the right LPM (Mine et al., 2008). In contrast, *Noggin* and *Chordin* are not expressed in the LPM of the chick embryo (Chapman et al., 2002; Streit and Stern, 1999) and no difference in pSMAD1 distribution between the right and left LPM can be detected (Supplementary Fig. S2). This conclusion is consistent with a previous report (Faure et al., 2002). How can similar levels of BMP signaling produce differences in the patterns of *Nodal* expression in each side of the LPM? One explanation is that there are other regulatory steps in addition to phosphorylation of SMADs. Recent reports have shown that BMP and ACTIVIN/NODAL signaling pathways antagonize each other through competition between pSMAD1 and pSMAD2 in binding to their common signaling component SMAD4 (Candia et al., 1997; Furtado et al., 2008; Yamamoto et al., 2009). On the basis of these observations, we hypothesized that a small change to the BMP signaling level might affect ACTIVIN/NODAL signaling via SMAD4 competition, leading to different levels of NODAL signaling in each side of the LPM.

We carried out various experiments to test our hypothesis on SMAD4 competition. These results obtained were consistent with our proposal that competition between pSMAD1 and pSMAD2 for SMAD4 regulates *Nodal* expression in the LPM of the chick embryo, in a similar fashion to the mouse embryo (Furtado et al., 2008). Small changes in BMP or NODAL signaling levels could shift the balance of the SMAD complexes in the LPM. In the chick embryo, *Bmp2*, *-4*, and *-7* are symmetrically expressed in the LPM during L–R axis formation (Monsoro-Burq and Le Douarin, 2000; Yokouchi et al., 1999). Consequently, BMP signaling is active and the pSMAD1/SMAD4 complex predominates in both sides of the LPM. In the presence of a low concentration of BMP in the left LPM, a low level of BMP signaling increases the amount of pSMAD1/SMAD4 complex but decreases the pSMAD2/SMAD4 complex. Under these conditions, the NODAL positive-feedback loop is maintained in a quiescent state despite the additional NODAL from the node. In the presence of a low concentration of NOGGIN in the right LPM, a small decrease in BMP signaling decreases the pSMAD1/SMAD4 complex and increases the pSMAD2/SMAD4 complex, thereby lowering the threshold for activation of the positive-feedback loop. In this case, the NODAL positive-feedback loop is activated even in the presence of a background level of NODAL.

A proposed mechanism for Nodal up-regulation by a high level of BMP signaling

Previous studies indicated that *Nodal* induction by a high concentration of BMP is an indirect effect mediated by the up-regulation of *Cfc*, a co-receptor for the NODAL receptor and a BMP

dependent gene in the LPM (Piedra and Ros, 2002; Schlange et al., 2001); the up-regulation of *Cfc* then sensitizes LPM cells to NODAL (Piedra and Ros, 2002; Schlange et al., 2002). We tested this proposal in various experiments. First, we showed that *Nodal* up-regulation by a high concentration of BMP4 (100 μg/ml) was completely suppressed by SB431542, an inhibitor of the ACTIVIN/NODAL receptor (Fig. 7C). This result indicates that *Nodal* induction by the high concentration of BMP was an indirect effect and depended on NODAL receptor signaling. Second, we demonstrated that overexpression of *Cfc* in the right LPM induced *Nodal* expression (Fig. 4C and C′), indicating that *Cfc* overexpression was sufficient for *Nodal* induction. Third, we found that SB431542 completely suppressed *Nodal* induction by *Cfc* overexpression (Fig. 7G and G′), suggesting that *Nodal* induction by *Cfc* overexpression depended on NODAL receptor signaling. Overall, these results support the proposal that a high concentration of BMP activates *Nodal* expression via up-regulation of *Cfc* expression which, in turn, leads to sensitization of the cells in the right LPM to NODAL (Piedra and Ros, 2002; Schlange et al., 2002).

Nodal induction by a high concentration of BMP4 was evident at HH7 but not at HH5 (Figs. 2 and 6). Treatment of embryos between HH4 and HH6 with a high concentration of BMP suppressed *Shh* expression in the node and abolished *Nodal* expression in the LPM (Monsoro-Burq and Le Douarin, 2001; Piedra and Ros, 2002). Interestingly, inhibition of SHH signaling by anti-SHH antibodies resulted in the absence of *Nodal* expression in the LPM, although it did not inhibit *Nodal* expression in the perinodal region (Raya and Izpisua Belmonte, 2008; Raya et al., 2004). These observations suggest that SHH signaling regulates the availability of NODAL from the node. Therefore, the NODAL ligand for induction of *Nodal* in the LPM would be unavailable in embryos treated with a high concentration of BMP4 between HH4 and HH6. In contrast, when a high concentration of BMP4 was applied at HH7, *Nodal* is induced. One possible explanation for *Nodal* induction at HH7 is that there are populations of cells expressing *Nodal* in the left LPM and that these provide the NODAL ligand. Although *Shh* expression in the node might be suppressed by BMP4, it appears to be no longer required for *Nodal* induction in the LPM at HH7.

Cfc expression and pSMAD1 are symmetrically distributed between the left and right LPMs during in vivo development. Thus, although high experimental concentrations of BMP can induce *Nodal* by up-regulating *Cfc* expression, these conditions are unlikely to occur in vivo.

Multiple effects of BMP signaling on Nodal expression

The proposal that L–R axis formation in the chick embryo is mediated by a mechanism that involves BMP regulation of *Nodal* expression is controversial. Here, we have obtained results that suggest a way to reconcile the contradictory conclusions of previous studies regarding the role of BMP signaling. We have identified four different dose-dependent effects of BMP signaling on *Nodal* expression (Fig. 8):

(1) When the BMP signaling level is high, *Nodal* expression is induced through *Cfc* up-regulation. This condition was achieved experimentally by application of high concentrations of BMP for implantation into each side of the LPM

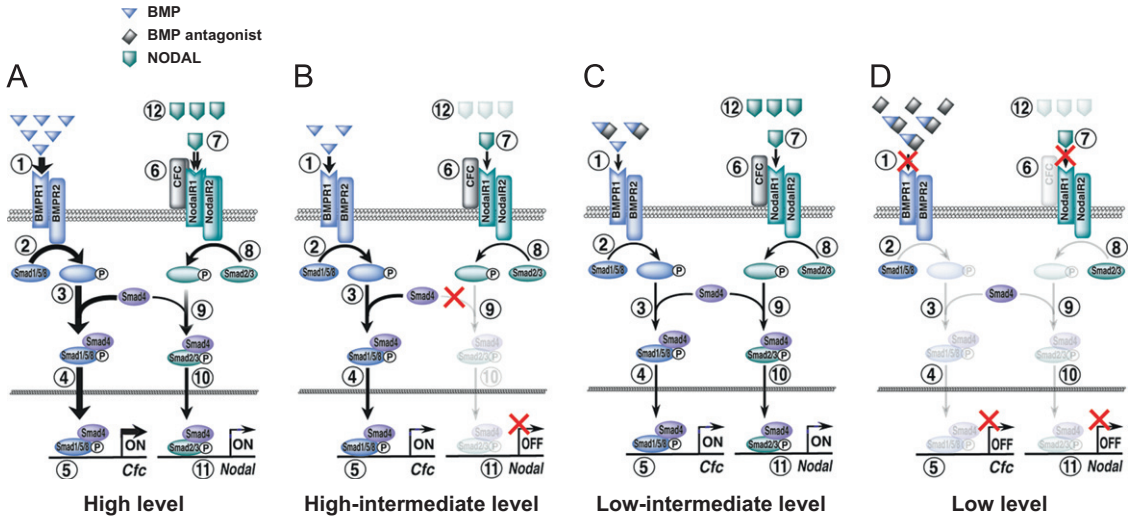

Fig. 8. Multi-modal effects of BMP signaling on *Nodal* expression: A model for the multiple roles of BMP signaling in *Nodal* expression. Variations in BMP signaling strength produce four different states of *Nodal* expression in the LPM. The thickness of the arrows represents the traffic quantity of each step. (A) High BMP signaling level. Steps 1–5: In the presence of a high concentration of BMP, *Cfc* expression is strongly activated. Step 6: Increased CFC production causes an increase in the sensitivity of the NODAL receptor to NODAL. Steps 7 and 8: NODAL at background level activates the NODAL receptor. Step 9: Increase in levels of pSMAD2/3 raises the probability of formation of pSMAD2/3-SMAD4 complexes. Steps 10–12: As a result, *Nodal* transcription and the NODAL positive-feedback loop are activated. This state is equivalent to an LPM with an experimentally applied high concentration of BMP. (B) High intermediate BMP signaling level. Steps 1 and 2: BMPs bind to and activate BMP receptors. Steps 3 and 4: pSMAD1/5/8 associate with SMAD4 and translocate to the nucleus. Step 5: pSMAD1/5/8-SMAD4 complexes stimulate expression of target genes including the NODAL co-receptor *Cfc*. Steps 6–10: At this level of BMP signaling, CFC production for NODAL binding to the receptor is maintained, and NODAL present at the basal level activates the NODAL receptor; however, the predominance of binding between pSMAD1/5/8 and SMAD4 causes a shortage of free SMAD4, preventing pSMAD2/3 forming a complex with SMAD4. Steps 11 and 12: As a result, *Nodal* transcription and the NODAL positive-feedback loop are inactivated. This state is equivalent to the native right LPM, or to the left LPM with an experimentally applied low concentration of BMP. (C) Low intermediate BMP signaling level. Steps 1–6: In the presence of a low concentration of the BMP antagonist, BMP binding to the receptor is weakly inhibited and free SMAD4 is released from pSMAD1/5/8-SMAD4 complexes, although *Cfc* expression is still maintained. Steps 7 and 8: NODAL from the node or present at the basal level binds to the receptor and activates the NODAL receptor. Steps 9 and 10: Phosphorylated SMAD2/3 associates with free SMAD4 and translocates to the nucleus. Steps 11 and 12: This activates *Nodal* transcription and the NODAL positive-feedback loop. This state is equivalent to the native left LPM, or to the right LPM with an experimentally applied with low concentration of a BMP antagonist. (D) Low BMP signaling level. Steps 1–5: In the presence of a high concentration of a BMP antagonist, BMP binding to the receptor and downstream events leading to *Cfc* expression are strongly inhibited. Steps 6–12: As a result of decreased CFC production, NODAL binding to the receptor and downstream events leading to *Nodal* expression and the NODAL positive-feedback loop are strongly inhibited. This state is equivalent to the LPM with an experimentally applied high concentration of a BMP antagonist such as NOGGIN.

(Piedra and Ros, 2002; Yu et al., 2008). At high concentration, BMP induced a high level of *Cfc* expression, which may have sensitized cells to NODAL ligand (normally present below the threshold level in the right LPM) and activated *Nodal* expression (Piedra and Ros, 2002).

(2) When BMP-pSMAD1/4 signaling is activated at a high intermediate level, the balance between NODAL-pSMAD2/4 and BMP-pSMAD1/4 signaling shifts toward BMP-pSMAD1/4 signaling. This switch inhibits activation of the NODAL positive feedback loop due to deficient amounts of the pSMAD2/4 complex. This condition may correspond to the physiological level of BMP-pSMAD1/4 signaling in the right LPM, as *Bmp2*, *-4*, and *-7* are bilaterally expressed in the LPM (Monsoro-Burq and Le Douarin, 2000; Yokouchi et al., 1999), and can be experimentally mimicked by application of a low concentration of BMP in the left LPM.

(3) When BMP-pSMAD1/4 signaling is inhibited and produces a low intermediate signaling level, the balance between NODAL-pSMAD2/4 and BMP-pSMAD1/4 signaling shifts toward NODAL-pSMAD2/4 signaling. This switch activates the NODAL positive feedback loop, although the level of BMP-pSMAD1/4 signaling is still sufficient to maintain *Cfc* expression. This condition may correspond to the physiological level of BMP-pSMAD1/4 signaling in the left LPM, and can be experimentally mimicked by application of a low concentration of NOGGIN to the right LPM.

(4) When the BMP-pSMAD1/4 signaling level is low, BMP-pSMAD1/4 signaling is strongly suppressed by a high concentration of a BMP antagonist. In this case, expression of *Cfc* is repressed, which in turn suppresses the NODAL positive feedback loop (Piedra and Ros, 2002). This condition can be experimentally induced by a high concentration of NOGGIN (Piedra and Ros, 2002; Yu et al., 2008).

Differential regulation of *Nodal* expression might occur at different developmental stages. BMP signaling at a high intermediate level may correspond to the embryo before and at HH5 because *Bmp* genes are expressed in the LPM whereas *Nodal* is not yet expressed. BMP signaling at a low intermediate level may correspond to the embryo at and after HH6 because perinodal expression of *Nodal* begins and NODAL protein moves into the left LPM. BMP signaling at a high or a low level may not be found in vivo, as discussed in the previous section.

In conclusion, our findings show that BMP signaling can display multiple effects with respect to *Nodal* expression in the LPM. Our data also suggest that the regulatory mechanism for *Nodal* expression by BMP signaling during L–R patterning is not a simple switch but a parallel circuit with a common mediator, SMAD4. This circuit might enable multiple expression patterns of *Nodal* in response to different concentrations of BMP. Crosstalk between BMP signaling and TGF-β signaling is crucial for patterning of the body axes, germ layer patterning in the embryonic stem cells, and differentiation of mesenchymal cells, such as C2C12, ATDC5, and MEFs (Candia et al., 1997; Furtado et al., 2008; Keller et al., 2011; Watabe and Miyazono, 2009; Wrighton et al., 2009; Yamamoto et al., 2009). We believe our new findings will aid in the understanding of the complicated spatio-temporal patterns of gene expression that are associated with cell differentiation during different aspects of development.

Acknowledgments

We are grateful to Drs. K. Miyazono (University of Tokyo) and T. Imamura (Ehime University) for kindly providing pc3-Alk4 (TD)-HA and pc3-Alk6 (QD)-HA, Dr. Y. Takahashi (Nara Institute of Science and Technology) for kindly providing pCAGGS and pCAGGS-GFP, and technical advice on electroporation in the chick embryo. K.K. thanks Drs. K. Matsumoto (MRC Centre for Developmental Neurobiology), T. Suzuki (Nagoya University), and Y. Igarashi (OLYMPUS software technology corp.) for discussion and technical advice. This work was mainly supported by a Grant-in-Aid for Scientific Research from the Ministry of Education, Science, Sports and Culture of Japan, in part by Grants-in-Aid for 21st Century COE Research from the Ministry of Education, Culture, Sports, Science and Technology 'Cell Fate Regulation Research and Education Unit'.

Appendix A. Supporting information

Supplementary data associated with this article can be found in the online version at: http://dx.doi.org/10.1016/j.ydbio.2012.11.027.

References

Affolter, M., Basler, K., 2007. The Decapentaplegic morphogen gradient: from pattern formation to growth regulation. Nat. Rev. Genet. 8, 663–674.
Candia, A.F., Watabe, T., Hawley, S.H., Onichtchouk, D., Zhang, Y., Derynck, R., Niehrs, C., Cho, K.W., 1997. Cellular interpretation of multiple TGF-beta signals: intracellular antagonism between activin/BVg1 and BMP-2/4 signaling mediated by Smads. Development 124, 4467–4480.
Chang, H., Zwijsen, A., Vogel, H., Huylebroeck, D., Matzuk, M.M., 2000. Smad5 is essential for left–right asymmetry in mice. Dev. Biol. 219, 71–78.
Chapman, S.C., Schubert, F.R., Schoenwolf, G.C., Lumsden, A., 2002. Analysis of spatial and temporal gene expression patterns in blastula and gastrula stage chick embryos. Dev. Biol. 245, 187–199.
Faure, S., de Santa Barbara, P., Roberts, D.J., Whitman, M., 2002. Endogenous patterns of BMP signaling during early chick development. Dev. Biol. 244, 44–65.
Fujiwara, T., Dehart, D.B., Sulik, K.K., Hogan, B.L., 2002. Distinct requirements for extra-embryonic and embryonic bone morphogenetic protein 4 in the formation of the node and primitive streak and coordination of left–right asymmetry in the mouse. Development 129, 4685–4696.
Furtado, M.B., Solloway, M.J., Jones, V.J., Costa, M.W., Biben, C., Wolstein, O., Preis, J.I., Sparrow, D.B., Saga, Y., Dunwoodie, S.L., Robertson, E.J., Tam, P.P., Harvey, R.P., 2008. BMP/SMAD1 signaling sets a threshold for the left/right pathway in lateral plate mesoderm and limits availability of SMAD4. Genes Dev. 22, 3037–3049.
Granata, A., Quaderi, N.A., 2003. The Opitz syndrome gene MID1 is essential for establishing asymmetric gene expression in Hensen's node. Dev. Biol. 258, 397–405.
Hamada, H., Meno, C., Watanabe, D., Saijoh, Y., 2002. Establishment of vertebrate left–right asymmetry. Nat. Rev. Genet. 3, 103–113.
Hamburger, V., Hamilton, H.L., 1992. A series of normal stages in the development of the chick embryo, 1951. Dev. Dyn. 195, 231–272.
Katsu, K., Tokumori, D., Tatsumi, N., Suzuki, A., Yokouchi, Y., 2012. BMP inhibition by DAN in Hensen's node is a critical step for the establishment of left–right asymmetry in the chick embryo. Dev. Biol. 363, 15–26.
Keller, B., Yang, T., Chen, Y., Munivez, E., Bertin, T., Zabel, B., Lee, B., 2011. Interaction of TGFbeta and BMP signaling pathways during chondrogenesis. PLoS One 6, e16421.
Kishigami, S., Yoshikawa, S., Castranio, T., Okazaki, K., Furuta, Y., Mishina, Y., 2004. BMP signaling through ACVRI is required for left–right patterning in the early mouse embryo. Dev. Biol. 276, 185–193.
Levin, M., Johnson, R.L., Stern, C.D., Kuehn, M., Tabin, C., 1995. A molecular pathway determining left-right asymmetry in chick embryogenesis. Cell 82, 803–814.
Mine, N., Anderson, R.M., Klingensmith, J., 2008. BMP antagonism is required in both the node and lateral plate mesoderm for mammalian left–right axis establishment. Development 135, 2425–2434.
Mizutani, C.M., Meyer, N., Roelink, H., Bier, E., 2006. Threshold-dependent BMP-mediated repression: a model for a conserved mechanism that patterns the neuroectoderm. PLoS Biol. 4, e313.
Monsoro-Burq, A., Le Douarin, N., 2000. Left–right asymmetry in BMP4 signalling pathway during chick gastrulation. Mech. Dev. 97, 105–108.
Monsoro-Burq, A., Le Douarin, N.M., 2001. BMP4 plays a key role in left–right patterning in chick embryos by maintaining Sonic Hedgehog asymmetry. Mol. Cell 7, 789–799.
Muller, P., Rogers, K.W., Jordan, B.M., Lee, J.S., Robson, D., Ramanathan, S., Schier, A.F., 2012. Differential diffusivity of Nodal and Lefty underlies a reaction–diffusion patterning system. Science 336, 721–724.
Nakao, A., Imamura, T., Souchelnytskyi, S., Kawabata, M., Ishisaki, A., Oeda, E., Tamaki, K., Hanai, J., Heldin, C.H., Miyazono, K., ten Dijke, P., 1997. TGF-beta

receptor-mediated signalling through Smad2, Smad3 and Smad4. Embo J. 16, 5353–5362.
Nakayama, M., Matsumoto, K., Tatsumi, N., Yanai, M., Yokouchi, Y., 2006. Id3 is important for proliferation and differentiation of the hepatoblasts during the chick liver development. Mech. Dev. 123, 580–590.
New, D.A.T., 1955. A new technique for the cultivation of the chick embryo in vitro. J. Embryol. Exp. Morphol. 3, 320–331.
Noro, M., Yuguchi, H., Sato, T., Tsuihiji, T., Yonei-Tamura, S., Yokoyama, H., Wakamatsu, Y., Tamura, K., 2011. Role of paraxial mesoderm in limb/flank regionalization of the trunk lateral plate. Dev. Dyn. 240, 1639–1649.
Onuma, Y., Yeo, C.Y., Whitman, M., 2006. XCR2, one of three Xenopus EGF-CFC genes, has a distinct role in the regulation of left–right patterning. Development 133, 237–250.
Piedra, M.E., Ros, M.A., 2002. BMP signaling positively regulates Nodal expression during left right specification in the chick embryo. Development 129, 3431–3440.
Psychoyos, D., Stern, C.D., 1996. Fates and migratory routes of primitive streak cells in the chick embryo. Development 122, 1523–1534.
Raya, A., Izpisua Belmonte, J.C., 2008. Insights into the establishment of left–right asymmetries in vertebrates. Birth Defects Res. C Embryo Today 84, 81–94.
Raya, A., Kawakami, Y., Rodriguez-Esteban, C., Ibanes, M., Rasskin-Gutman, D., Rodriguez-Leon, J., Buscher, D., Feijo, J.A., Izpisua Belmonte, J.C., 2004. Notch activity acts as a sensor for extracellular calcium during vertebrate left–right determination. Nature 427, 121–128.
Rodriguez Esteban, C., Capdevila, J., Economides, A.N., Pascual, J., Ortiz, A., Izpisua Belmonte, J.C., 1999. The novel Cer-like protein Caronte mediates the establishment of embryonic left–right asymmetry. Nature 401, 243–251.
Schlange, T., Arnold, H.H., Brand, T., 2002. BMP2 is a positive regulator of Nodal signaling during left–right axis formation in the chicken embryo. Development 129, 3421–3429.
Schlange, T., Schnipkoweit, I., Andree, B., Ebert, A., Zile, M.H., Arnold, H.H., Brand, T., 2001. Chick CFC controls Lefty1 expression in the embryonic midline and nodal expression in the lateral plate. Dev. Biol. 234, 376–389.
Shen, M.M., 2007. Nodal signaling: developmental roles and regulation. Development 134, 1023–1034.
Shiratori, H., Hamada, H., 2006. The left–right axis in the mouse: from origin to morphology. Development 133, 2095–2104.
Streit, A., Stern, C.D., 1999. Establishment and maintenance of the border of the neural plate in the chick: involvement of FGF and BMP activity. Mech. Dev. 82, 51–66.
Tabin, C.J., 2006. The key to left–right asymmetry. Cell 127, 27–32.
Tavares, A.T., Andrade, S., Silva, A.C., Belo, J.A., 2007. Cerberus is a feedback inhibitor of Nodal asymmetric signaling in the chick embryo. Development 134, 2051–2060.
Watabe, T., Miyazono, K., 2009. Roles of TGF-beta family signaling in stem cell renewal and differentiation. Cell Res. 19, 103–115.
Wrighton, K.H., Lin, X., Yu, P.B., Feng, X.H., 2009. Transforming growth factor {beta} can stimulate Smad1 phosphorylation independently of bone morphogenic protein receptors. J. Biol. Chem. 284, 9755–9763.
Yamamoto, M., Beppu, H., Takaoka, K., Meno, C., Li, E., Miyazono, K., Hamada, H., 2009. Antagonism between Smad1 and Smad2 signaling determines the site of distal visceral endoderm formation in the mouse embryo. J. Cell Biol. 184, 323–334.
Yang, X., Dormann, D., Munsterberg, A.E., Weijer, C.J., 2002. Cell movement patterns during gastrulation in the chick are controlled by positive and negative chemotaxis mediated by FGF4 and FGF8. Dev. Cell 3, 425–437.
Yokouchi, Y., Vogan, K.J., Pearse 2nd, R.V., Tabin, C.J., 1999. Antagonistic signaling by Caronte, a novel Cerberus-related gene, establishes left–right asymmetric gene expression. Cell 98, 573–583.
Yu, X., He, F., Zhang, T., Espinoza-Lewis, R.A., Lin, L., Yang, J., Chen, Y., 2008. Cerberus functions as a BMP agonist to synergistically induce nodal expression during left–right axis determination in the chick embryo. Dev. Dyn. 237, 3613–3623.
Zhu, L., Marvin, M.J., Gardiner, A., Lassar, A.B., Mercola, M., Stern, C.D., Levin, M., 1999. Cerberus regulates left–right asymmetry of the embryonic head and heart. Curr. Biol. 9, 931–938.